Acoustic phonon modulation of terahertz quantum cascade lasers

A. Demić*, A. Valavanis*, J. Bailey†, P. Dean*,
L. H. Li*, A. G. Davies*, E. H. Linfield*, P. Harrison‡, J. E. Cunningham*, A. Kent†

* School of Electronic and Electrical Engineering, University of Leeds, Leeds LS2 9JT, UK
† School of Physics and Astronomy, University of Nottingham, Nottingham NG7 2RD, UK
‡ School of Computing and Engineering, University of Huddersfield, Huddersfield HD1 3DH, UK
e-mail: A.Demic@leeds.ac.uk

INTRODUCTION

We investigate theoretical methods for the analysis of acoustic phonon modes in arbitrary heterostructure superlattice and their effect on modulating transport in terahertz-frequency quantum-cascade lasers (THz QCLs). We solve the acoustic phonon wave equation via Fourier method to obtain excellent agreement with experimental results (Fig. 1-3). Our model is applicable to arbitrary heterostructure profile. The acoustic stop-bands in a THz QCL were measured via an ultrafast pump–probe spectroscopy technique, using a pair of mode-locked Ti:Sapphire Tsunami femtosecond lasers, tuned to a wavelength of 810 nm. We use the envelope of the obtained acoustic deformation potential as a perturbation to bandstructure potential (Fig. 4) to analyse electron transport in common THz QCLs active-region design schemes via density matrix approach [1]. We find that acoustic modes up to $\sim$200 GHz are capable of significantly perturbing QCL transport (Fig. 5-6), highlighting their potential for ultra-fast modulation of laser emission. This agrees well with our demonstration by using externally generated acoustic pulses [2].

ACOUSTIC PHONON MODE MODELLING

We consider the acoustic wave equation [3]: $\frac{\partial}{\partial z}v_s^2(z)\frac{\partial}{\partial z}\psi(z,t) - \frac{\partial^2}{\partial t^2}\psi(z,t) = 0$ where $\psi(z,t)$ is the acoustic wave pressure and $v_s(z)$ is the acoustic velocity. This equation can be solved using a Fourier method, by assuming $\psi(z,t) = \psi_0\psi_n(z)\exp(-i\omega_n t)$, where ψ_0 is the wave amplitude, ω_n the angular frequency and $p_n(z)$ the envelope of the acoustic wave:

$$-\frac{\partial}{\partial z}v_s^2(z)\frac{\partial}{\partial z}p_n(z) = \omega_n^2 p_n(z) \qquad (1)$$

which can be discretised via finite-difference method. The obtained envelopes of the resonant phonon modes $p_n(z)$ are directly proportional to the local acoustic strain, and this can be added as a static deformation potential $V_{S_n}(z)$ to the Hamiltonian for an electron in the QCL:

$$V_{S_n}(z) = M \cdot p_n(z) \qquad (2)$$

where M is a modulation strength constant.

REFERENCES

[1] A. Demić *et.al*, AIP Advances 9 no. 9, 095019 (2019).
[2] A. Dunn *et.al*, Nature communications 11 no. 1, 1 (2020).
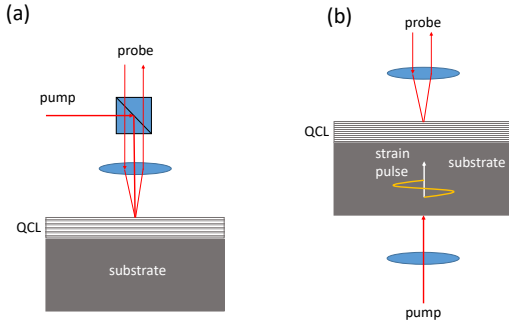[3] P. Harrison and A. Valavanis, John Wiley & Sons, (2016).

Fig. 1: Schematic illustrations of ASOPS experimental configurations, showing (a) reflection mode, and (b) transmission mode geometries.
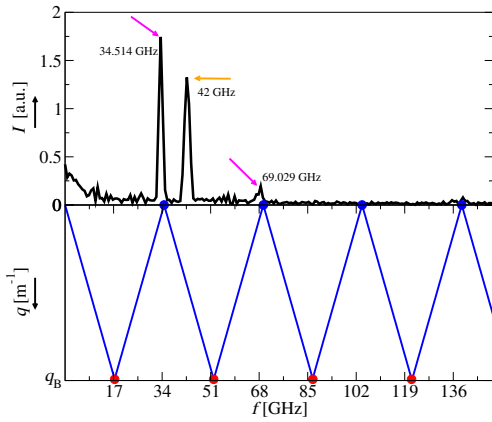

Fig. 2: Experimental probe reflectivity spectrum (top), obtained using a reflection-mode ASOPS geometry, and folded dispersion of the first Brillouin zone (bottom), obtained by solving Eq. (1) for a single period of the Hybrid THz QCL [2].
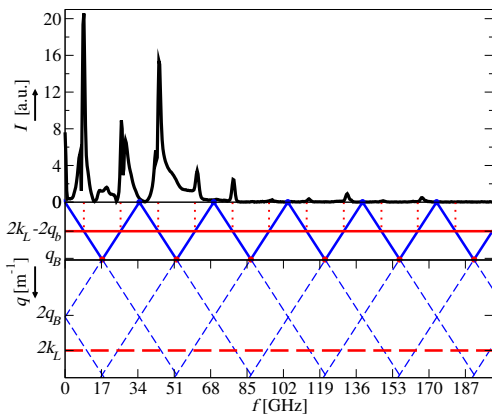

Fig. 3: Experimental probe reflectivity spectrum (top), using the transmission-mode ASOPS geometry, and acoustic dispersion resulting from model in Equation (1) (bottom). Solid blue lines represent the phonon dispersion, folded into the first Brillouin zone. The red dashed line corresponds to $q = 2k_L$, and the red solid line shows this folded into the first phonon Brillouin zone.
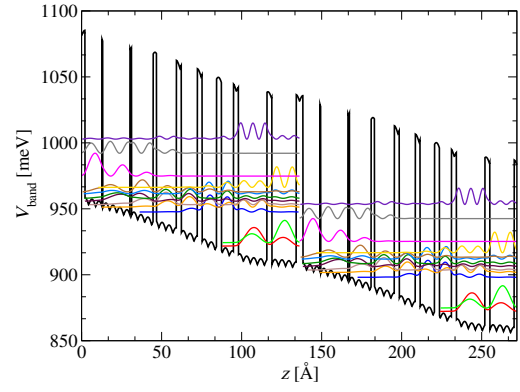

Fig. 4: Conduction band potential of a hybrid QCL design [2] with the addition of the 30th acoustic mode with modulation $M = 5$ meV. Two periods are shown at the resonance bias $K = 3.63 \frac{kV}{cm}$ along with the corresponding wavefunction moduli squared.
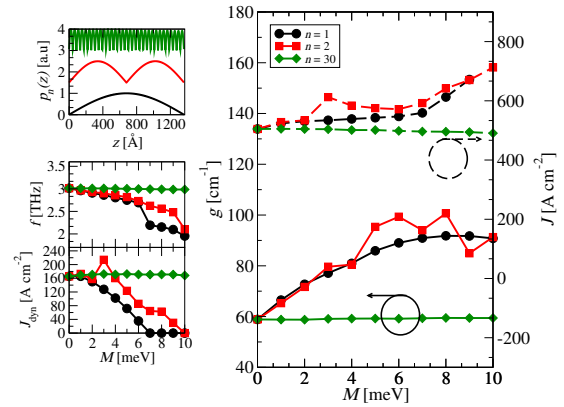

Fig. 5: Top inset: acoustic strain perturbation for mode index $n = 1, 2, 30$. Bottom insets: Frequency dependence (at NDR point) and dynamic range dependence, respectively, on modulation strength M for $n = 1, 2, 30$. Graph on the right: Full line traces illustrate material gain peaks from figure in a) as modulation M is varied for $n = 1, 2, 30$, while dashed lines illustrate current density peaks (NDR points) of the Hybrid THz QCL [2].
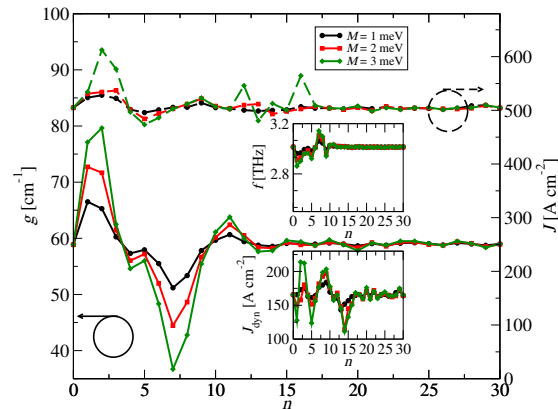

Fig. 6: Dependence of performance parameters for Hybrid THz QCL [2], as a function of acoustic mode index, using varying modulation strengths $M = 1, 2, 3$ meV. Results are shown for (a) emission frequency (at NDR point), (b) dynamic range, (c) peak gain, and (d) current density at the NDR point.